Human Parasitic Diseases

HYPOTHESIS

Computational Characterization of Surface-Associated Binding Interaction of Alpha-Enolase of *Trichomonas vaginalis* with Human Plasminogen

Surya Prakash Dwivedi[1,2], Nuzhat Husain[1] and GV Reddy[2]

[1]Genetics Laboratory, Department of Pathology, CSM Medical University, Lucknow-226003, India. [2]Department of Parasitology, Postgraduate Institute of Medical Education and Research, Chandigarh-160 012, India.
Corresponding author email: drnuzhathusain@hotmail.com

Abstract: *Trichomonas vaginalis* is a parasitic protozoan causing the most common human sexually transmitted disease (STD), trichomoniasis. The exact mechanism of its pathogenesis is still obscure. Alpha-enolase plays a pivotal role in the host-pathogen interaction, and as a surface receptor of several protists mediating plasminogen binding. In view of identifying plasminogen binding sites of *T. vaginalis* alpha-enolase, homology modeling and docking studies were conducted to obtain modeled structures of the *T. vaginalis* alpha-enolase-plasminogen complex. Modeling templates were searched by using BLAST, followed by multiple sequence alignment. The atomic coordinates of *Escherichia coli* enolase was retrieved from Protein Data Bank. Molecular structures of *T. vaginalis* alpha-enolase were modeled by using restraint-based modeling, followed by energy minimization using MODELLER program. The quality and stereochemistry of the models were evaluated by program PROCHECK. After addition of Mg^{2+}, the selected model further refined by energy minimization employing NAMD program. The VMD program was used to superimpose structure of *T. Vaginalis* alpha-enolase model with crystal structures of enolases from *E. coli* and *S. pneumoniae*. *T. vaginalis* alpha-enolase model was docked to human plasminogen for protein-protein interaction using Hex 5.1. Mark Gerstein's calc-surface program was used to calculate the solvent accessibility at the interface of *T. vaginalis* alpha-enolase and human plasminogen before and after docking. The finding provides new insights for interaction at the protein-protein interface. Our theoretical prediction is consistent with preexisting biochemical data. The predicted interaction complex can be of great assistance in understanding structural insights, probably being necessary to an interaction between pathogen and host-component. The ability of *T. vaginalis* alpha-enolase to bind plasminogen may be indicative of being a key player in invasion of this pathogen to host. Conclusively, this work theoretically establishes the *T. vaginalis* alpha-enolase as a novel surface-linked virulence factor.

Keywords: *Trichomonas vaginalis,* alpha-enolase, human plasminogen, MODELLER, NAMD, HEX, protein-protein interaction

Human Parasitic Diseases 2011:3 1–10

doi: 10.4137/HPD.S5601

This article is available from http://www.la-press.com.

Introduction

Human trichomoniasis is one of the major non-viral sexually transmitted disease caused by protozoan parasite *Trichomonas vaginalis*. It causes vaginitis, urethritis and cervicits. It also causes complains include premature labor, low birth weight offspring and post abortion pelvic inflammatory disease in women.[1] Worldwide, there are 250 million new cases of trichomoniasis is reported.[2] The infection in women may be asymptomatic or symptomatic leading to high risk of HIV (human immunodeficiency virus) infection.[3] A serological study links between trichomoniasis with prostate cancer.[4] For the significant human morbidity caused by *T. vaginalis*, there is a need for identifying virulence factors and elucidating the pathogenesis mechanisms of disease. Alpha-enolase is one of the secreted surface-associated protein which have binding domain interacting with human plasminogen.[5–7]

The first step of *T. vaginalis* infection is the colonizing of parasite in to vaginal epithelial cells. In a study surface-associated adhesin proteins were shown to be responsible for parasite adherence to vaginal epithelial cells (VECs).[8–10] In a separate study a direct relationship between the amount of surface adhesin and level of cytoadherence leads to binding of host cells in a ligand-receptor type interaction.[10,11] Interaction of host cells with VECs produces a morphological change by synthesizing the adhesions.[12,13]

Patients, suffering from persistent *T. vaginalis* infection are a continuous transmission source to others in their community.[14] A number of recently developed therapies are no longer effective treatments.[15] Indeed, the mechanism underlying the virulence of the pathogen is known very little. In case of asymptomatic subjects, it is still obscure. A study of the mechanisms adopted by *T. vaginalis* to invade and survive within host cells was carried out using confocal laser scanning microscopy indicating that *T. vaginalis* has advanced mechanisms, which are not phagocytosis, for entering host cells.[15,16] It was suggested that *Mycoplasma* species invaded host cells by adhering to the surface of host cells and later move across the membrane into host cells.[17] A proposed mechanism, based on several studies, involved in pathogenesis is the interaction of parasite cells with the human plasminogen system. The study demonstrated that binding of *T. vaginalis* energize plasminogen.[18–20]

Studies pertain to α-enolase-plasminogen complexes have clearly shown that receptor-bound plasminogen is more readily converted to plasmin than free plasminogen.[21,22] Enolase was characterized, by using competitive plasminogen binding assays and cross-linking studies with 125I-labeled plasminogen and intact streptococci, as a plasminogen receptor on the surface of streptococc.[21] This investigation clearly showed that enolase significantly contributed to overall ability of *Streptococcus* to bind plasminogen. In a manner similar to that of streptococci, enolase mediated the binding of *Candida albicans* to plasminogen, which increased ability of cells in crossing in vitro human brain microvascular endothelial cells.[17] Recently, there have been a number of reports indicating that enolase enhances the virulence of some pathogens.[16] The microbial enolase is captured by human plasminogen, and its subsequent conversion to plasmin provides a mechanism to augment virulence, favoring host tissue invasion.[23–25]

For such action, enolase protein must be located on the surface of microbial pathogens.[21,25] The matrix-assisted laser desorption ionization-time of flight mass spectrometry (MALDI-TOF MS) analysis of the peptide sequence of *Streptococcus mutans* enolase revealed possibility of phosphorylation site(s).[25] These findings suggested that enolase phosphorylation might occur and lead to its translocation to pathogen's cell surface. In addition, immunogold bead staining supported the MALDI-TOF MS finding that enolase was detected on the surface of *S. mutans*.[25] The secreted enolase reassociates with the bacterial cell surface was confirmed by direct binding of radiolabeled recombinant protein to pneumococci and by field emission scanning electron microscopic analysis.[23,26] The *M. fermentans* α-enolase binding to plasminogen has recently been reported.[27–29] In light of the above findings, this work is an attempt to predict molecular interaction of *T. vaginalis* enolase with human plasminogen by computational modeling which would be useful for further investigation of the mechanism of *T. vaginalis* invasion to vaginal epithelial cells (VECs).

Methodology

The protein sequence of *T. vaginalis* alpha-enolase used in this study was kindly provided by Dr. John F. Alderete (University of Texas, USA). Modeling

templates were searched by using BLAST, followed by multiple sequence alignment. In order to analyze modeled complex of protein-protein interaction, sequence identity of 40%–50% between target and template may be required. The atomic coordinates of *Saccharomyces cerevisiae* enolase (PDB ID: 2AL1) was retrieved from Protein Data Bank. Molecular structures of *T. vaginalis* alpha-enolase were modeled by using restraint-based modeling, followed by energy minimization using MODELLER program (Python program: model-ligand.py).[30] Several models were generated and were then energy minimized using the molecular dynamics and simulation procedure CHARMM[31] in program MODELLER. The quality and stereochemistry of the models were evaluated using the program PROCHECK.[32] The final model was selected based on stereochemical quality. The main-chain conformations for 98.80% amino acid residues were within the favored or allowed regions of the Ramachandran plot and the overall G-factor was -0.11, indicating that molecular geometry of the model is of good quality. The selected model was then added Mg^{2+} and further refined by energy minimization by the NAMD program (http://www.ks.uiuc.edu/Research/namd/) by 2,000 steps of conjugate gradient minimization until the energy gradient RMS was <0.05 kcal (mol Å)-1. Structural models were visualized by PyMol™ Molecular Graphics System version 0.97 (DeLano Scientific LLC, San Carlos, CA, USA, http://www.pymol.org). The quality and stereochemistry of the models were evaluated by program PROCHECK.[33] After addition of Mg^{2+}, the selected model further refined by energy minimization employing NAMD program. The VMD program was used to superimpose structure of *T. Vaginalis* alpha-enolase model with crystal structures of enolases from *E. coli* (PDB ID: 1E9I)[34] and *S. pneumoniae* (PDB ID: 1W6T).[35] *T. vaginalis* alpha-enolase model was docked to human plasminogen for protein-protein interaction using Hex 5.1 (http://www.csd.abdn.ac.uk/hex/). An automated energy minimization was applied for each docking solution. But no action was performed. The atomic coordinates of human plasminogen was retrieved from PDB (PDB ID: 1B2I).[36] Automate energy minimization was applied to each docking solution. The Chimera program (http://www.cgl.ucsf.edu/chimera/) was exploited to identify hydrogen bonds using default parameters and geometric criteria described previously.[37] Mark Gerstein's calc-surface program was used to calculate the solvent accessibility at the interface of *T. vaginalis* alpha-enolase and human plasminogen before and after docking.

Results and Discussion

Template identification and model quality

Crystal structures of enolases from many organisms, including those from bacteria, have already been determined and available in PDB.[27,34] Based on sequence similarity analysis, *T. vaginalis* enolase shows 55% amino acid sequence identity with *Saccharomyces cerevisiae* enolase. It is one of top ranks with high degree of sequence identities between *T. vaginalis* enolase and other enolases with known structures. Practically, at this level of sequence identity, it is good enough to use crystallographic structures of *Saccharomyces cerevisiae* enolase as a template, in order to obtain high quality alignment for structure prediction by homology modeling. An *Saccharomyces cerevisiae* crystal structure 2AL1[34] was specifically selected on the basis of BLAST result and was utilized as a template for *T. vaginalis* enolase structure modeling. Structural models for *T. vaginalis* enolase were built by MODELLER program (Python program: model-ligand.py)[30] based on atomic coordinates of 2AL1 and were then energy minimized. The model with the lowest objective function (2875.0945 kcal/mol) with DOPE SCORE of –48688.945313 kcal/mol, which was considered as the best one, was selected and subjected to quality evaluation.

The PROCHECK Ramachandran plot analysis shows that the main-chain conformations for 90% of amino acid residues are within the most favored or allowed regions (Fig. 1). The structural model of *T. vaginalis* enolase is shown in Figure 3a. The G-factors, indicating the quality of covalent and bond angle distance, were –0.04 for dihedrals, –0.27 for covalent, and overall –0.12. The overall main-chain and side-chain parameters, as evaluated by PROCHECK, are all very favorable.[33,35,38,39] The comparable Ramachandran plot characteristic and G-factors confirm the quality of predicted model. The *T. vaginalis* enolase model consists of typical two domains. The N-terminal one contains three-stranded antiparallel β-sheets, followed by six α-helices. The C-terminal domain composes of eleven-stranded mixed α/β-barrel with connectivity. The

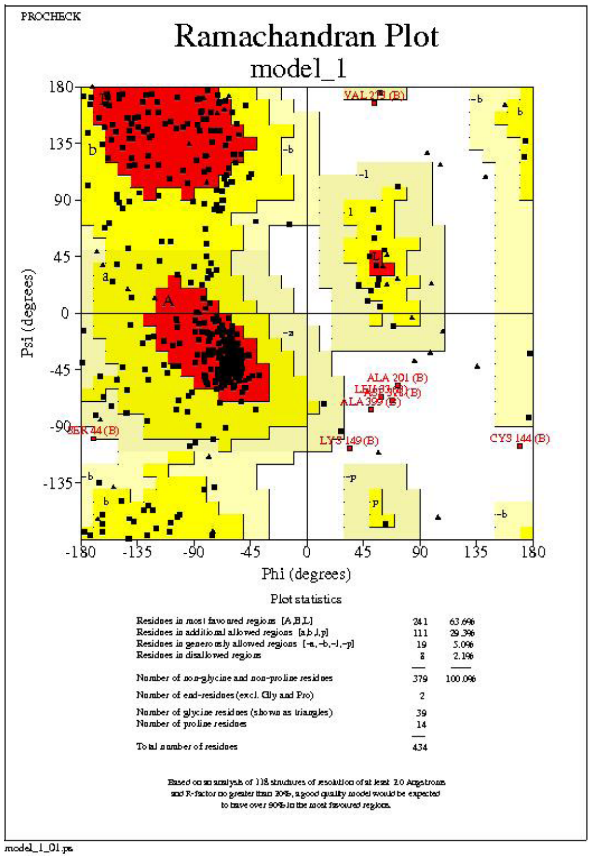

Figure 1. Ramachandran plot for theoretical model of *T. vaginalis* enolase.

first α-helix within the C-terminal domain, H7, and the second β-strand, S7, of the barrel domain were arranged in an antiparallel fashion compared to all other α-helices and β-strands (Fig. 2). The RMSD (Root Mean Square Deviation) between predicted model and template is 0.4 Å (Angstrom). The overall conformation of *T. vaginalis* enolase model is similar to those of *E. coli* enolase and *S. pneumoniae* enolase crystal structures[27,34] as observed by the superposition analysis shown in Figure 2. The Mg^{2+}, a metal ion cofactor, was encircled by Asp256, Glu310, and Asp337 which located in active site of enolase

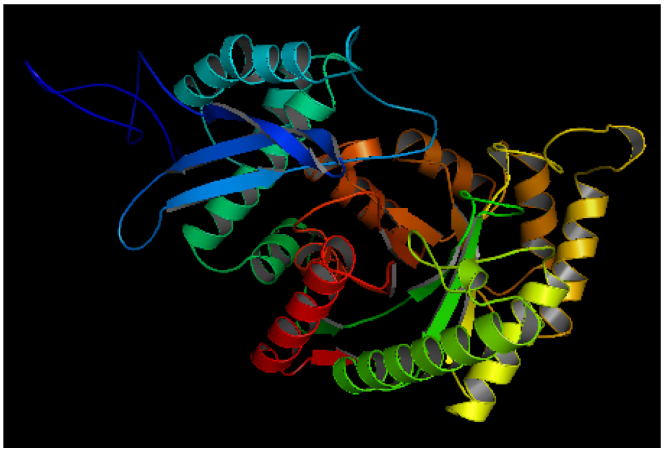

Figure 2. Theoretical model of *M. pneumoniae* enolase. This model was conducted by MODELLER program. Overall structure of *T. vaginalis* enolase with containing Mg^{2+} cofactor.

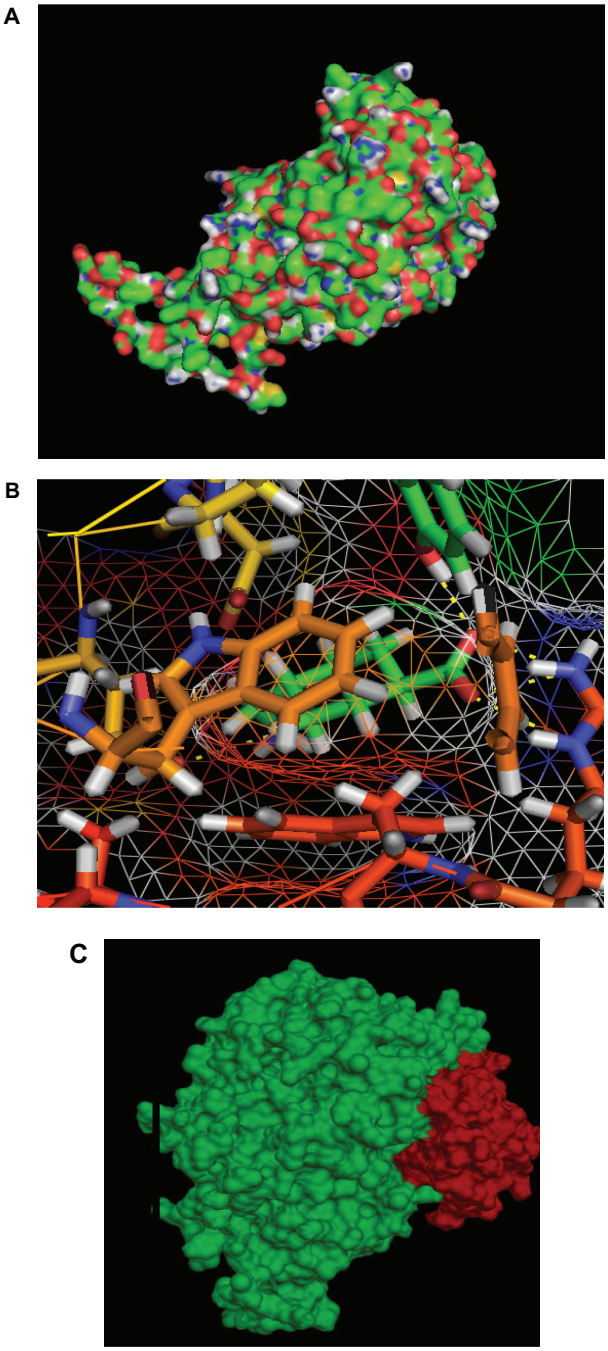

Figure 3. Model of *T. vaginalis* enolase-human plasminogen complex interaction. **A**) H-bond represent in red line. **B**) Electrostatic surfaces, a color ramp was calculated, which positive potential charges in blue, negative values in red, and intermediate values in white by using PyMol (http://pymol.sourceforge.net/). **C**) *T. vaginalis* enolase interaction with human plasminogen.

(Fig. 3a). Although Mg^{2+} is required for catalytic activity of the enzyme, it may also play a role in stabilizing enolase conformation.[34]

Interaction of *M. pneumoniae* enolase and human plasminogen

Based on rigid-body docking using HEX 5.1, both proteins were analyzed for shape complementary, hydrophobic effects resulting from a decrease in the solvent accessible surface, and electrostatic interactions. The key amino acid residues within the docking complex model involved in the interaction between enolase (e) and human plasminogen (pg) are eLys70-pgTyr50, eAsn165-pgThr66, eAla168-pgGlu21, eAsp17-pgLys70, and eAsn213-pgPro68/pgAsn69 (Fig. 3b. These residues were determined based on intermolecular hydrogen bond lengths of amino acid residues interacted between human plasminogen and *T. vaginalis* enolase. All hydrogen bond lengths appear to be shorter than 3.4 Å (Table 1 under supplementary material). This suggests that hydrogen bonds can be plausibly formed. The docking result indicated that the complex could be stabilized by hydrogen bonding. Electrostatic potential surface area showed that 10 amino acid residues of *T. vaginalis* enolase appeared to be available for making contact with plasminogen (Fig. 3c). These also include eArg24, eLys70, and eLys216, positive charge residues located at the opposite end of the binding pocket. On human plasminogen molecule, several charge amino acid residues, including pgGlu21, pgAsp26, and pgAsp67, appeared in electrostatic potential surface area. Moreover, the decreases of accessible surface area (ΔASA) of the docking complex were observed Table 2a and Table 2b (see supplementary material). Considering *T. vaginalis* enolase, significant change of accessible surface area of eLys70 occurred. Noticeably, hydrogen bonding was observed on this residue. For human plasminogen on the complex, the model showed large decrease in accessible surface area involving residues pgGlu21, pgTyr50, pgAsp67, pgPro68, pgAsn69 and pgLys70. Some of these appeared to form hydrogen bonds with corresponding residues of *T. vaginalis* enolase. The results suggest that model of the interaction complex between *T. vaginalis* enolase and human plasminogen can be practicable.

Our model of *T. vaginalis* enolase-plasminogen complex was in agreement with the previous study lysine binding site (LBS) of plasminogen in terms of charge characteristics.[40] In addition, the proposed interaction between human plasminogen and *T. vaginalis* enolase agreed with previous experimental investigations.[24,25,27] The interaction between human plasminogen and *T. vaginalis* enolase proposed in this study is useful for understanding the possible mechanism used by *T. vaginalis* to invade veginal epithelial cells (VECs). For instance, the interaction between human plasminogen and *T. vaginalis* enolase might provide a vehicle for targeting cells. This line of work may lead to insight into host-pathogen interaction and provide valuable information for prophylactic strategies in combating infections at a very early stage.

Conclusion

The rationale in building a *T. vaginalis* enolase model and performing a binding study with human plasminogen is to gain details of interaction between the two proteins. *T. vaginalis* enolase modeling was conducted using homology modeling. Comparison of the obtained model with experimentally derived crystal structures of *E. coli* enolase and *S. pneumoniae* enolase revealed that they were all basically similar. The docking studies revealed the important residues involving in the interaction of *T. vaginalis* enolase with human plasminogen. Analyses of the interaction model between human plasminogen and *T. vaginalis* enolase, based on distances of hydrogen bonds, changes of solvent accessible surface, electrostatic potentials, showed that this binding complex was reliable. Our theoretical prediction may lead to the establishment of prophylactic and therapeutic approaches.

Acknowledgements

The authors are grateful to Prof. Nancy Malla, Professor and Head, Department of Parasitology, PGIMER, Chandigarh for providing the necessary facilities and encouragement. The protein sequence of *T. vaginalis* alpha-enolase used in this study was kindly provided by Dr. John F. Alderete (University of Texas, USA). The authors are also thankful to Prof. R.M. Dubey (Managing Director) IFTM, Moradabad, U.P., India and Prof. A. Srivastav (Director), College of Engineering and Technology, Moradabad, U.P., India, for providing an institutional research promotion grant and their

generous help and encouragement during the course of experimental work and manuscript preparation.

Disclosure

This manuscript has been read and approved by all authors. This paper is unique and is not under consideration by any other publication and has not been published elsewhere. The authors and peer reviewers of this paper report no conflicts of interest. The authors confirm that they have permission to reproduce any copyrighted material.

References

1. World Health Organization, Three hundred, thirty-three million new, STD curable cases in 1995. *AIDS Wkly*. 1995:15–16.
2. Cates W Jr; The American Social Health Association Panel. Estimates of the incidence and prevalence of sexually transmitted diseases in the United States. *Sex Transm Dis*. 1999;26:S2–7.
3. Sorvillo F, Smith L, Kerndt P, Ash L. *Trichomonas vaginalis,* HIV and African-Americans. *Emerg Infect Dis*. 2001;7:927–32.
4. Sutchiffe S, Giovannueci E, Alderete JF, et al. Plasma antibodies against *Trichomonas vaginalis* and subsequent risk of prostate cancer. *Cancer Epidemiol Biomarkers Prev*. 2006;15:939–45.
5. Kucknoor AS, Mundodi V, Alderete JF. Adherence to human vaginal epithelial cells signals for increased expression of *Trichomonas vaginalis* genes. *Infect Immun*. 2005;73:6472–8.
6. Mundodi V, Kucknoor AS, Klumpp DJ, Chang TH, Alderete JF. Silencing the *ap65* gene reduces adherence to vaginal epithelial cells by *Trichomonas vaginalis*. *Mol Microbiol*. 2004;53:1099–108.
7. Mundodi V, Kucknoor AS, Alderete JF. Antisense RNA decreases AP33 gene expression and cytoadherence by *T vaginalis. BMC Microbiol*. 2007;3:64.
8. Alderete JF, Obrien JL, Arroyo R, et al. Cloning and molecular characterization of two genes encoding adhesion proteins involved in *Trichomonas vaginalis* cytoadherence. *Mol Microbiol.* 1995;17:69–83.
9. Engbring JA, Alderete JF. Characterization of *Trichomonas vaginalis* AP33 adhesin and cell surface interactive domains. *Microbiology*. 1998;144: 3011–18.
10. Garcia AF, Chang TH, Benchimol M, Klumpp DJ, Lehker MW. Alderete JF. Iron and contact with host cells induce expression of adhesins on surface of *Trichomonas vaginalis*. *Mol Microbiol*. 2003;47:1207–24.
11. Arroyo R, Engbring J, Alderete JF. Molecular basis of host epithelial cell recognition by *Trichomonas vaginalis Mol Microbiol*. 1992;6:853–62.
12. Arroyo R, Gonzalez-Robles A, Martinez-Palomo A, Alderete JF. Signaling of *Trichomonas vaginalis* for amoeboid transformation and adhesin synthesis follows cytoadherence. *Mol Microbiol*. 1993;7:299–309.
13. Kucknoor AS, Mundodi V, Alderete JF. Heterologous expression in *Tritrichomonas foetus* of functional *Trichomonas vaginalis* AP65 adhesin. *BMC Mol Biol*. 2005;6:5.
14. Mundodi V, Kucknoor AS, Alderete JF. Immunogenic and Plasminogen-Binding Surface-Associated α-Enolase of *Trichomonas vaginalis Infect Immun*. 2008;76:2:523–31.
15. Abonyi A. Examination of non flagellate and flagellate round forms of *Trichomonas vaginalis* by transmission electron microscopy. *Appl Parasitol*. 1995;36:303–310.
16. Alderete JF. Antigen analysis of several pathogenic strains of *Trichomonas vaginalis*. *Infect Immun*. 1983;39:1041–7.
17. Arroyo R, Alderete JF. *Trichomonas vaginalis* surface proteinase activity is necessary for parasite adherence to epithelial cells. *Infect Immun*. 1989;57:2991–7.
18. Yavlovich A, Tarshis M, Rottem S. Internalization and intracellular survival of *Mycoplasma pneumoniae* by non-phagocytic cells. *FEMS Microbiol Lett*. 2004;233:241.
19. Pancholi V, Chhatwal GS. Housekeeping enzymes as virulence factors for pathogens. *J Med Microbiol*. 2003;293:391.
20. Jong AY, Chen SH, Stins MF, Kim KS, Tuan TL, Huang SH. Binding of *Candida albicans* enolase to plasminogen results in enhanced invasion of human brain microvascular endothelial cells. *J Med Microbiol*. 2003;52:615.
21. Yavlovich A, Katzenell A, Tarshis M, Higazi AA, Rottem S. Mycoplasma fermentans binds to and invades HeLa cells: involvement of plasminogen and urokinase. *Infect Immunol*. 2004;72:5004.
22. Yavlovich A, Higazi AA, Rottem S. Plasminogen binding and activation by Mycoplasma fermentans. *Infect Immunol*. 2001;69:1977.
23. Lottenberg R, Minning-Wenz D, Boyle MD. Capturing host plasminogen: a common mechanism for invasive pathogens? *Trend Microbiol*. 1994;2:20.
24. Pancholi V, Fischetti VA. Alpha-enolase, a novel strong plasmin(ogen) binding protein on the surface of pathogenic streptococci. *J Biol Chem*. 1998; 273:14503.
25. Redlitz A, Fowler BJ, Plow EF, Miles LA. The role of an enolase-related molecule in plasminogen binding to cells. *Eur J Biochem*. 1995;227:407.
26. Fox D, Smulian AG. Plasminogen-binding activity of enolase in the opportunistic pathogen. *Pneumocystis carinii Med Mycol*. 2001;39:495 (2001).
27. Bergmann S, Rohde M, Chhatwal GS, Hammerschmidt S. Alpha-Enolase of *Streptococcus pneumoniae* is a plasminogen-binding protein displayed on the bacterial cell surface. *Mol Microbiol*. 2001;40:1273.
28. Ge J, Catt DM, Gregory RL. Streptococcus mutans surface alpha-enolase binds salivary mucin MG2 and human plasminogen. *Infect Immun*. 2004;72: 6748.
29. Yavlovich A, Rechnitzer H, Rottem S. Alpha-enolase resides on the cell surface of *Mycoplasma fermentans* and binds plasminogen. *Infect Immunol*. 2007;75:5716.
30. Sali A, Potterton L, Yuan F, van Vlijmen H, Karplus M. Evaluation of comparative protein modeling by MODELLER. *Proteins*. 1995;23:318.
31. Sali A, Blundell TL. Comparative protein modelling by satisfaction of spatial restraints. *J Mol Biol*. 1993;234:779.
32. Morris AL, MacArthur MW, Hutchinson EG, Thornton JM. Stereochemical quality of protein structure coordinates. *J Appl Cryst*. 1993;26:283.
33. Laskowski RA, MacArthur MW, Moss DS, Thornton JM. PROCHECK: a program to check the stereochemical quality of protein structures. *J Appl Cryst*. 1993;26:283–91.
34. Kühnel K, Luisi BF. Crystal structure of the Escherichia coli RNA degradosome component enolase. *J Mol Biol*. 2001;313:583.
35. Morris AL, MacArthur MW, Hutchinson EG, Thornton JM. Stereochemical quality of protein structure coordinates. *Proteins*. 1992;12:345–64.
36. Marti DN, Schaller J, Llinás M. Solution structure and dynamics of the plasminogen kringle 2-AMCHA complex: 3(1)-helix in homologous domains. *Biochemistry*. 1999;38:15741.
37. Mills JE, Dean PM. Three-dimensional hydrogen-bond geometry and probability information from a crystal survey. *J Comput Aided Mol Des*. 1996;10:607.
38. Kabsch W, Sander C. Dictionary of protein secondary structure: pattern recognition of hydrogen-bonded and geometrical features. *Biopolymers*. 1983;22:2577–637.
39. Nishikawa K, Ooi T. Radial locations of amino-acid residues in a globular protein—correlation with the sequence. *J Biochem*. 1986;100:1043–7.
40. Gong Y, Kim SO, Felez J, Grella DK, Castellino FJ, Miles LA. Conversion of Glu-plasminogen to Lys-plasminogen is necessary for optimal stimulation of plasminogen activation on the endothelial cell surface. *J Biol Chem*. 2001;276:19078.

Supplementary Material

Table S1. The distance between the modeled *M. pneumoniae* enolase and human plasminogen bound by hydrogen bonding.

***T. vaginalis* enolase**	**Human plasminogen**	**Distance (Å)**
Lys70-NZ	Tyr50-OH	2.68
Asn165-ND2	Thr66-O	3.21
Ala168-O	Glu21-N	3.21
Asp171-OD1	Lys70-NZ	3.24
Asn213-ND2	Pro68-O	1.93
Asn213-OD1	Asn69-ND2	2.94

Table S2a. Accessible Surface Area (ASA) values of the amino acids of the *M. pneumoniae* enolase model that made contact or produced hydrogen bonding with human plasminogen.

***T. vaginalis* enolase amino acid residue**	**ASA of free *T. vaginalis* enolase**	**ASA of *M. pneumoniae* enolase + plasminogen**
Arg24	37.14	19.41
Phe26	24.14	9.61
Lys70	22.96	4.08*
Asn165	0.94	0.94*
Ala168	21.27	3.17*
Asp171	38.34	38.34*
Asn213	23.43	23.43*
Thr214	25.05	25.05
Asn215	33.49	33.49
Lys216	19.44	19.44
Asp218	5.84	5.63

Note: *Hydrogen bond produced.

Table S2b. Accessible Surface Area (ASA) values of the amino acid of human plasminogen that made contact or produced hydrogen bonding with the modeled *T. vaginalis enolase.*

Plasminogen amino acid residue	**ASA of plasminogen**	**ASA of plasminogen + *M. pneumoniae* enolase**
Glu21	21.81	3.45*
Asp26	9.49	3.43
Ser27	16.11	14.553
Gln28	25.92	7.59
Ser29	20.21	11.35
Pro30	15.50	6.66
Lys48	34.70	0.80
Tyr50	18.76	4.13*
Thr66	21.35	21.09*
Asp67	12.66	0.70
Pro68	30.78	7.75*
Asn69	40.05	20.20*
Lys70	27.32	1.27*

Note: *Hydrogen bond produced.

Appendix 3
Stereochemical parameters
The two tables in this appendix list the stereochemical parameters used in the *PROCHECK programs.*

Table 3A. Stereochemical parameters of Morris et al. (1992), derived from high-resolution protein structures.

Stereochemical parameter	Mean value	Standard deviation
Phi-psi in most favored regions of Ramachandran plot	>90%	
chi1 dihedral angle:		
Gauche minus	64.1 degrees	15.7 degrees
Trans	183.6 degrees	16.8 degrees
Gauche plus	–66.7 degrees	15.0 degrees
chi2 dihedral angle	177.4 degrees	18.5 degrees
Proline phi torsion angle	–65.4 degrees	11.2 degrees
Helix phi torsion angle	–65.3 degrees	11.9 degrees
Helix psi torsion angle	–39.4 degrees	11.3 degrees
chi3 (S–S bridge)		
right-handed	96.8 degrees	14.8 degrees
left-handed	–85.8 degrees	10.7 degrees
Disulphide bond separation	2.0 A	0.1 A
omega dihedral angle	180.0 degrees	5.8 degrees
Main-chain hydrogen bond energy (kcal/mol)*	–2.03	0.75
C alpha chirality: zeta "virtual" torsion angle C_{alpha}–N–C–C_{beta}	33.9 degrees	3.5 degrees

Note: *Evaluated using the Kabsch and Sander (1983) method.

Table 3B. Main-chain bond lengths and bond angles, and their standard deviations, as observed in small molecules (Engh and Huber, 1991). The atom-labelling follows that used in the x-plor dictionary, with some additional atom types (marked with an asterisk) as defined by Engh and Huber (1991).

a. Bond lengths

Bond sigma	X—PLOR labeling		Value	
C–N	$C–NH_1$	(except Pro)	1.329	0.014
	C–N	(Pro)	1.341	0.016
C–O	C–O		1.231	0.020
$C_{alpha}–C$	$CH_1E–C$	(except Gly)	1.525	0.021
	$CH_2G^*–C$	(Gly)	1.516	0.018
$C_{alpha}–C_{beta}$	$CH_1E–CH_3E$	(Ala)	1.521	0.033
	$CH_1E–CH_1E$	(Ile, Thr, Val)	1.540	0.027
	$CH_1E–CH_2E$	(the rest)	1.530	0.020
$N–C_{alpha}$	$NH_1–CH_1E$	(except Gly, Pro)	1.458	0.019
	$NH_1–CH_2G^*$	(Gly)	1.451	0.016
	N–CH1E	(Pro)	1.466	0.015

b. Bond angles

Angle sigma	X—PLOR labeling		Value	
$C–N–C_{alpha}$	$C–NH_1–CH_1E$	(except Gly, Pro)	121.7	1.8
	$C–NH_1–CH_2G^*$	(Gly)	120.6	1.7
	C–N–CH1E	(Pro)	122.6	5.0
$C_{alpha}–C–N$	$CH_1E–C–NH_1$	(except Gly, Pro)	116.2	2.0
	$CH_2G^*–C–NH_1$	(Gly)	116.4	2.1
	$CH_1E–C–N$	(Pro)	116.9	1.5
$C_{alpha}–C–O$	$CH_1E–C–O$	(except Gly)	120.8	1.7
	$CH_2G^*–C–O$	(Gly)	120.8	2.1
$C_{beta}–C_{alpha}–C$	$CH_3E–CH_1E–C$	(Ala)	110.5	1.5
	$CH_1E–CH_1E–C$	(Ile, Thr, Val)	109.1	2.2
	$CH_2E–CH_1E–C$	(the rest)	110.1	1.9
$N–C_{alpha}–C$	$NH_1–CH_1E–C$	(except Gly, Pro)	111.2	2.8
	$NH_1–CH_2G^*–C$	(Gly)	112.5	2.9
	$N–CH_1E–C$	(Pro)	111.8	2.5
$N–C_{alpha}–C_{beta}$	$NH_1–CH_1E–CH_3E$	(Ala)	110.4	1.5
	$NH_1–CH_1E–CH_1E$	(Ile, Thr, Val)	111.5	1.7
	$N–CH_1E–CH_2E$	(Pro)	103.0	1.1
	$NH_1–CH_1E–CH_2E$	(the rest)	110.5	1.7
O–C–N	$O–C–NH_1$	(except Pro)	123.0	1.6
	O–C–N	(Pro)	122.0	1.4

Appendix B

Brookhaven file format

The table below shows the Brookhaven file format for the coordinate records (ie, ATOM and HETATM) of your .pdb file. Each record holds the coordinates and other details of a single atom.

Field no.	Column range	FORTRAN format	Description
1	1–6	A6	Record ID (eg ATOM, HETATM)
2	7–11	I5	Atom serial number
–	12–12	1X	Blank
3	13–16	A4	Atom name (eg “CA”, “ND1”)
4	17–17	A1	Alternative location code (if any)
5	18–20	A3	Standard 3-letter amino acid code for residue
–	21–21	1X	Blank
6	22–22	A1	Chain identifier code
7	23–26	I4	Residue sequence number
8	27–27	A1	Insertion code (if any)
–	28–30	3X	Blank
9	31–38	F8.3	Atom’s x-coordinate
10	39–46	F8.3	Atom’s y-coordinate
11	47–54	F8.3	Atom’s z-coordinate
12	55–60	F6.2	Occupancy value for atom
13	61–66	F6.2	B-value (thermal factor)
–	67–67	1X	Blank
14	68–68	I3	Footnote number